

Fatigue Life Estimation Using Single Spot-Welded Joint Fracture Mechanics

Bhimrao Pawal¹, Krishan Pandey², Chetan Chimote³, Pushpaketan Deotale⁴,
Shanteshwar Dhanure⁵

Lecturer, Department of Mechanical Engineering^{1,2,3,4,5}
Pimpri Chinchwad Polytechnic, Pune, Maharashtra, India

Abstract: *The influence of a spot-welded joint on the overlap section of the specimen, which is critical for spot welded joints subjected to uniaxial in plane loads, on fatigue life is explored in this study. This study was carried out using the ANSYS finite element program. The fatigue life properties of spot-welded specimens with various gap values are numerically calculated using a created computer program and several fatigue-life techniques to see how the gap affects the fatigue life of the spot-welded specimens. With rising gap values, it is noticed that maximum stress and strain values increase, resulting in a loss in fatigue life. Maximum stresses and strains, and hence fatigue-life values, are shown to be relatively constant for gap values less than 0.0025mm.*

Keywords: Fatigue Life, Resistance Spot Welding, Finite Element Analysis, etc.

I. INTRODUCTION

Despite the trend toward other joining methods such as laser-beam welding, adhesive bonding, bolted and riveted joints, resistance spot welding (RSW) remains the primary joining method for joining or fastening panels and bodies that contain hundreds, if not thousands, of spot welds, especially in the automotive, railroad, and aero plane industries. The welding procedure is used in industrial applications because it provides excellent operating efficiency at a lower cost of production than other welding processes like laser and friction stir welding. Resistance spot welding, on the other hand, entails cutting a sharp slit into the welded joint, which increases stress concentration and causes the joint to shatter. In order to analyze the long-term strength reliability of spot-welded structures, it is necessary to first understand their fatigue properties. Spot welds in real cars are subjected to a variety of loads, including shear, peel, and cross tension. As a result, some articles have published spot-welded joint strength evaluation results under these stress conditions. Because the strength of spot-welded joints is known to be dependent on the type of metal used. The objective of this paper is to find stress-strain values of the specimen using finite element analysis and Fatigue life estimation of the specimen using different approaches.

II. LITERATURE REVIEW

A. H. Eartas, Y. Yilmaz, C. Baykara, the influence of the space or gap value between the overlap portions of components on fatigue life is explored in this study for two different types of geometry, MTS and TS, and for five different gap values. Fatigue lifetimes for five different gap values of MTS and TS specimens are computed using a computer software created by the authors utilising monotonic test data combined with empirical relationships found in the literature. They demonstrate that stress distributions generated under varied loading circumstances are realistic and exhibit a variety of characteristics. Because all stress and strain data at crucial places are available, they provide numerical capacity for fatigue analysis. The gap value between the overlap sections of the specimens is discovered to be significant and has an impact on the specimen's fatigue life.

Xiangbo Liu, Yanhong Wei, Haijiang Wu, Tao Zhang, to obtain the total residual deformation in continuous simulation, a 3-D comparison between the original geometry and the final deformed geometry is necessary, which can highlight the deformation interaction between the continuous welding processes. The virtual and actual welded rear side panels show good agreement in terms of deformation, demonstrating the direct

reliability of direct finite element analysis while modelling the resistance spot welding process. It also shows how parameter optimization through reverse engineering and direct finite element analysis is sensible. The reverse stamped pieces that make up the BSP are shown to have considerable clearances after assembly. The apparent deformation in the reverse BSP is caused by clamp pressure, electrode pressures, and residual tensile stresses.

Ryota Tanegashima, Hiroyuki Akebono, Atsushi Sugeta, the empirically obtained fatigue fracture initiation angles in this work deviated substantially from the conclusions of traditional theories on mixed-mode cracks in the locations most impacted by stress. Because the experimental and numerical results were so close, the theories' relevance to the fatigue properties of real joints appears to be dubious. Numerical methods, on the other hand, may be able to precisely predict the fatigue crack start angles of spot-welded joints. The fatigue properties of shear- and peel-type single spot-welded joints were examined experimentally and analytically to evaluate the accuracy of joint fatigue life calculations produced using traditional theories. The observed fracture start angles deviated from expectations based on traditional theories, implying that the theories cannot be used to assess the fatigue properties of the joints.

Sajjad Seifoori, Ahmad Mahdian Parrany, Mojtaba Khodayari, Fatigue fracture is one of the most common causes of failure in many rotating machinery components. In this paper, the fatigue behaviour of a typical shaft, which is widely used in the turbocharger of BELAZ 75131 mining dump trucks, is studied both theoretically and experimentally. There is one diameter change along the shaft and investigations show that the dominant cause of failure is fatigue caused by cyclic loadings. Finite element based numerical simulations are also performed by MSC Fatigue software to demonstrate the accuracy of the experimental results. In addition, a fatigue testing machine is developed to obtain the fatigue life of the shaft experimentally and validate the theoretical results.

Sendong Ren, Yunwu Ma, Shuhei Saeki, Yoshiaki Iwamoto, Chuantong Chen, Ninshu Ma, Coaxial one-side resistance spot welding was used to fuse carbon fibre reinforced polymers (CFRP) and Al5052 sheets. During the SLS test, the joints with low welding current showed interfacial fracture with low strength and little displacement, whereas the joints with high welding current showed a staged failure process with CFRP tearing, resulting in higher strength and bigger displacement. In welded junctions, molten CFRP produces a thin layer. It is always partially attached to the metal sheet. Micro gaps on the interface can be removed using a higher welding current. Excessive heat input, on the other hand, will cause ablation of the CFRP resin matrix.

III. IMPLEMENTATION

In the literature, there are stress-based and strain-based approaches to fatigue life estimation models. Because of the very confined plastic deformation around the spot weld nuggets, stress-based techniques were found to be more conservative for spot-weld joints. Only strain-based models with the best correlation with experimental results are used to evaluate fatigue life of spot-welded joints in this study.

$$\begin{aligned} \frac{\Delta \epsilon}{2} = \epsilon_a = \epsilon_e + \epsilon_p &= \frac{\Delta \epsilon_e}{2} + \frac{\Delta \epsilon_p}{2} \\ &= \frac{\sigma'_f}{E} (2N_f)^b + \epsilon'_f (2N_f)^c \end{aligned}$$

Where ϵ_e is the elastic component of the cyclic strain amplitude, ϵ_p the plastic component of the cyclic strain amplitude, ϵ'_f the regression intercept called 'the fatigue ductility coefficient', c the regression slope called 'the fatigue ductility exponent', σ'_f the regression intercept called 'the fatigue strength coefficient', N_f the number of cycles to failure, and b the regression slope called 'the fatigue strength exponent'

Experimentation is used to establish the most trustworthy results of fatigue behavior of structures, components, or elements. Empirical relations, developed by numerous researchers, are employed in the absence of experimentally determined values. Muralidharan and Manson relation, given by, is one of the most important empirical relations

$$\frac{\Delta \epsilon}{2} = \epsilon_a = 0.623 \left(\frac{s_{ut}}{E} \right)^{0.832} (2N_f)^{-0.09} + 0.0196 (\epsilon_p)^{0.155} \left(\frac{s_{ut}}{E} \right)^{-0.53} (2N_f)^{-0.56}$$

IV. NUMERICAL ANALYSIS

In numerical analysis, for the modelling of the MTS and TS specimens, following true stress versus strain curve, shown in Figure, is used

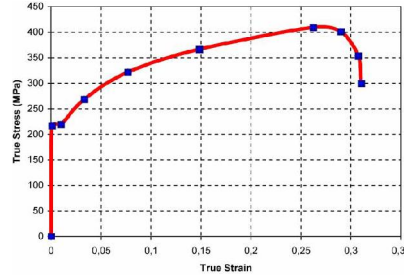


Figure 1: True stress versus strain curve

Initially, the space or gap value between the overlap portions of pieces is assumed as 0.02mm. Then the gap values (that is 0.01, 0.005, 0.0025, and 0.001 25 in mm) the analysis are repeated.

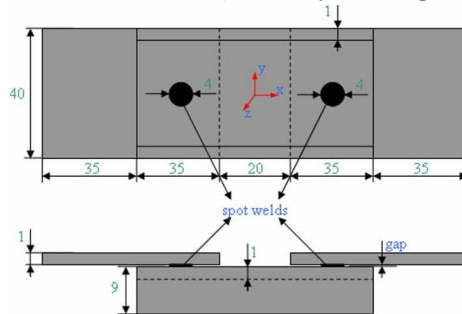


Figure 2: Geometry of MTS specimen (top and side views)

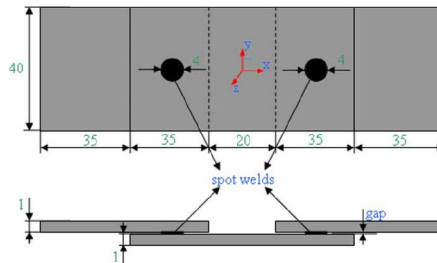


Figure 3: Geometry of TS specimen (top and side views)

A linear (two node) beam element in three-dimensional, BEAM188, is chosen for the description of the spot weld. When defining the mesh sizes, the influence of the mesh size on the resulting forces is analysed and the final elements sizes are defined after convergence.

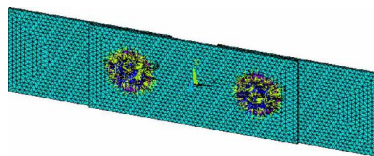


Figure 4: Finite-element model for TS specimen

The results of the convergence are shown In Tables 1 and 2 in terms of both material element size and sub steps versus first principal stress value for the load range of 150–2700N as an example.

Tables 1: Sub steps versus First principal stress value

Number of sub steps	First principal stress value(MPa)
10	486.34
20	443.6
40	420.72
80	415.47
120	414.5
160	412.94
200	412.6
240	412.2
320	415.72
640	418.22
1280	418.68
2560	418.69

Tables 2: Element size versus First principal stress value

Element size	First principal stress value(MPa)
0.012	248.59
0.007	278.42
0.005	312.21
0.004	355.55
0.003	380.67
0.0025	409.24
0.002	412.94
0.0015	413

V. BOUNDARY CONDITIONS

On the surface of the left end of the MTS and TS, all displacements and rotations of the associated nodes are fixed. Aside from that, all displacements and rotations of the associated nodes on the surface of the right end of the MTS and TS specimens are limited, with the exception of the 'x' (applied load) direction. The loading, on the other hand, is mimicked by applying negative pressure to a set of nodes on the areas of the right end's surfaces of MTS and TS specimens in cycles (to generate a tension effect). Because the distributions of nodes on surfaces are not uniform due to the specimen modelling, pressure is employed instead of load directly in the cycles.

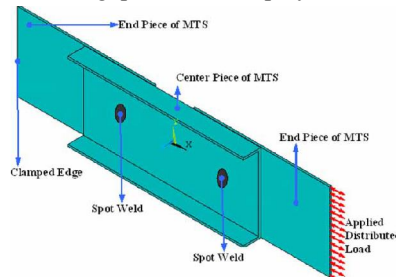


Figure 5: Boundary Conditions

VI. ANALYSIS AND FATIGUE LIFE CALCULATION

For proper design, stress concentration values must be as lower as possible in order to increase fatigue life values. Because the stress distributions of the TS and MTS specimens under loading conditions are similar the effect of solution type on stress concentration have been examined only for MTS specimen.

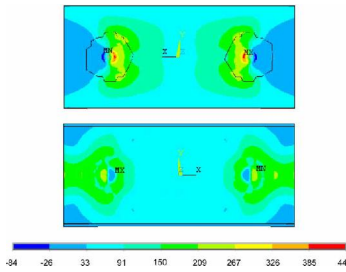


Figure 6: Distribution of principal true stress (in MPa) on the inner and outer surfaces of the central piece of the MTS specimen developed due to the maximum load (nodal type solution)

The minimum (150N) and maximum (3000N) loads are used to create these stresses. The fatigue life was calculated using a nodal solution in this study. A non-linear finite-element analysis is used to calculate the stress and strain values of the crucial nodes of spot-welded MTS and TS specimens. Under linearly elastic circumstances, a detailed analysis of the three-dimensional mechanical behavior of spot-welded joints was carried out for MTS and TS specimens. For MTS and TS specimens, finite-element solutions of the stress fields in the base metal and nugget have been derived.

VII. RESULT AND DISCUSSION

Figures show typical spot-weld fatigue results for two distinct types of geometry and five different gap values, according to various fatigue life prediction methodologies. Using a non-linear finite-element analysis, the stress and strain values of the critical nodes of spot-welded MTS and TS specimens for various gap values, namely 0.02, 0.01, 0.005, 0.0025, and 0.001 25 in mm, are estimated first. The fatigue life (number of cycles to failure) versus load range relations are then generated utilizing several types of fatigue life prediction algorithms.

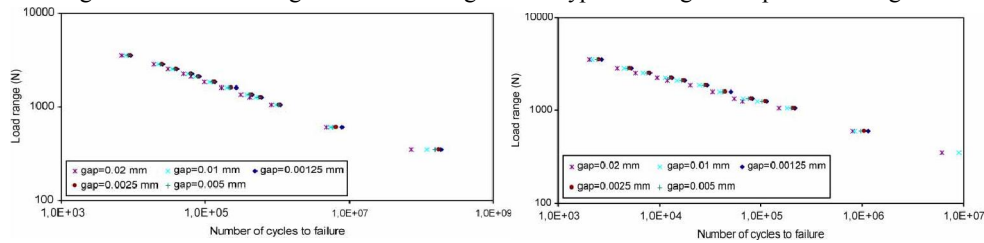


Figure 7: Results of fatigue analysis for different gap values of spot-welded MTS & TS specimen using the Coffin–Manson’s approach

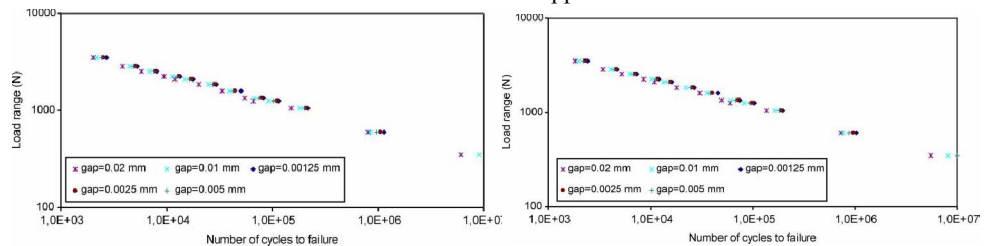


Figure 8: Results of fatigue analysis for different gap Values of spot-welded MTS & TS specimen using the Muralidharan and Manson’s Universal slopes approach

Variation of the number of cycles to failure versus gap value for the MTS specimen is obtained using fatigue lives calculated previously for the load range of 150–2700 N, as an example, and shown in Table 3 to clearly see the effect of the gap value between the overlap portions of the spot-welded specimens on fatigue life.

Gap value (mm)	Number of cycles to failure
0.02	30431
0.01	35128

0.005	38000
0.0025	39231
0.00125	40099

Table 3: Variation of the fatigue lives with respect to gap values for the spot-welded MTS specimen and load range of 150–2700 N

VIII. CONCLUSION

The influence of the spacing or gap value between the overlap portions of pieces on fatigue life is explored in this study for two different types of geometry, MTS and TS, as well as five various gap values. The created computer programme calculates fatigue lifetimes for five distinct gap values of MTS and TS specimens. The stress distributions obtained for various loading circumstances are realistic and exhibit a variety of distinguishing characteristics. Because all stress and strain data at crucial places are available, they provide numerical capacity for fatigue analysis. The gap value between the overlap sections of the specimens is discovered to be significant and has an impact on the specimen's fatigue life. The maximum stresses and strains decrease as the gap value decreases, resulting in an increase in fatigue life. Maximum stress and strains, and hence fatigue life values, do not change substantially for gap values less than 0.0025mm, especially for spot welded MTS specimens.

REFERENCES

- [1] AHErtas,YYilmaz, and C Baykara, “Aninvestigation of the effect of the gap values between the overlap portions of the spot-welded pieces on fatigue life”, Proceedings of the Institution of Mechanical Engineers, Part C: Journal of Mechanical Engineering Science(2008).
- [2] XiangboLiua, YanhongWeia, Haijiang Wub, Tao Zhangb, “Factor analysis of deformation in resistance spot welding of complex steelsheets based on reverse engineering technology and direct finite elementanalysis”, Journal of Manufacturing Processes 57 (2020) 72–90.
- [3] RyotaTanegashima, Hiroyuki Akebono, Atsushi Sugeta, “Fatigue Life Estimationbased on Fracture Mechanics of Single Spot-WeldedJoints under Different Loading Modes”, Engineering Fracture Mechanics(2017).
- [4] Sendong Ren, Yunwu Maa, Shuhei Saeki, Yoshiaki Iwamoto, Chuantong Chen, Ninshu Maa’ “Fracture mechanism and strength evaluation of Al5052/CFRP joint producedby coaxial one-side resistance spot welding”, Composite Structures 252 (2020) 112766.
- [5] S. Aslanlar, A. Ogur, U. Ozsarac, E. IlanWelding time effect on mechanical properties of automotive sheets in electrical resistance spot weldingMater Des, 29 (2008), pp. 1427-1431.
- [6] X. Kong, Q. Yang, B. Li, G. Rothwell, R. English, X.J. Ren Numerical study of strengths of spot-welded joints of steel Mater Des, 29 (2008), pp. 1554-1561.
- [7] H. Moshayedi, I. Sattari-Far Resistance spot welding and the effects of welding time and current on residual stresses J Mater Process Technol, 214 (2014), pp. 2545-2552.
- [8] J. Pakkanen, R. Vallant, M. Kicin Experimental investigation and numerical simulation of resistance spot welding for residual stress evaluation of DP1000 steel Weld World, 60 (2016), pp. 393-402.